Published in final edited form as:
Semin Nucl Med. 2014 September ; 44(5): 398–409. doi:10.1053/j.semnuclmed.2014.05.004.

Noninvasive Imaging in Coronary Artery Disease

Ran Heo[*], **Ryo Nakazato**[†], **Dan Kalra**[*], and **James K. Min, MD, FACC**[*]

[*]Dalio Institute of Cardiovascular Imaging, New York-Presbyterian Hospital and the Weill Cornell Medical College, New York, NY.

[†]St. Luke's International Hospital, Tokyo, Japan.

Abstract

Noninvasive cardiac imaging is widely used to evaluate the presence of coronary artery disease. Recently, with improvements in imaging technology, noninvasive imaging has also been used for evaluation of the presence, severity, and prognosis of coronary artery disease. Coronary CT angiography and MRI of coronary arteries provide an anatomical assessment of coronary stenosis, whereas the hemodynamic significance of a coronary artery stenosis can be assessed by stress myocardial perfusion imaging, such as SPECT/PET and stress MRI. For appropriate use of multiple imaging modalities, the strengths and limitations of each modality are discussed in this review.

Introduction

Coronary artery disease (CAD) is one of the leading causes of death, and the prevalence has increased worldwide.[1-3] To diagnose and define the severity of CAD, various imaging modalities have been introduced. For choosing the appropriate test, we review the strengths and limitations of each modality. Available modalities include the following: coronary CT angiography (CCTA), CT perfusion (CTP), computed fractional flow reserve (FFR) derived from CT (FFR_{CT}), nuclear myocardial perfusion imaging (MPI) (SPECT/PET), and cardiac MRI (CMR).

Coronary CT Angiography

As coronary revascularization is the main approach to treat CAD, CAD imaging has often been driven by the evaluation of anatomical stenosis severity. For this anatomical approach toward CAD, CCTA has gained its value with a rich evidence base that supports its clinical utility. In 3 prospective multicenter studies, the diagnostic performance of a 64-slice CCTA was reported in various populations.[4-6] The assessment by coronary computed tomographic angiography of individuals undergoing invasive coronary angiography (ACCURACY) trial was a 16–U.S. center study in patients without known CAD. The sensitivity, specificity, positive predictive value (PPV), and negative predictive value (NPV) of CCTA to detect ≥70% stenosis were 94%, 83%, 48%, and 99%, respectively.[4] The coronary artery

Address reprint requests to James K. Min, MD, FACC, Dalio Institute of Cardiovascular Imaging, New York-Presbyterian Hospital and the Weill Cornell Medical College, 520 E 70th St, New York, NY 10021. jkm2001@med.cornell.edu.

evaluation using a 64-row multidetector CT angiography (CORE64) study followed the ACCURACY trial as another multicenter study that was conducted in 291 patients both with and without known CAD who had baseline coronary artery calcium score less than 600 Agatston units. In this study, the per-patient sensitivity, specificity, PPV, and NPV for detecting ≥50% stenosis were 85%, 90%, 91%, and 83%, respectively. Furthermore, evaluation of stenosis using CCTA demonstrated that an area under the curve (AUC) was 0.91 for high-grade anatomical stenosis for invasive coronary angiography (ICA)–confirmed CAD, and it was similar to that demonstrated by ICA for the prediction of subsequent coronary artery revascularization.[5] In a third multicenter trial with 360 patients without known CAD presenting with both acute and stable chest pain, the CAD prevalence (≥50% stenosis) was high (68%), and diagnostic performance of CCTA was maintained, demonstrating a per-patient sensitivity, specificity, PPV, and NPV of 99%, 64%, 86%, and 97%, respectively.[6] The NPV for CCTA has generally been high (eg, 95%-100% in the 2 multicenter studies that constrained enrollment to those individuals without known CAD).[4,6,7] Based on these results, CCTA is now generally considered as a valuable tool for the exclusion of significant CAD.[8,9]

In addition to coronary stenosis severity, CCTA enables the study of other important atherosclerotic plaque characteristics with generally high accuracy. As an example, CCTA offers the diagnostic ability to assess measures of arterial remodeling, plaque composition, presence of intraplaque calcification, and aggregate plaque volume. Of these, positive arterial remodeling, low attenuation plaque, and spotty intraplaque calcification have shown a relation to both presently occurring and future acute coronary syndrome.[10-14] Plaque volume on CCTA determined by manual methods demonstrates a high correlation and a modest agreement with that determined by intravascular ultrasound.[12,15,16]

CCTA findings of CAD also inform measures of risk stratification in both asymptomatic and symptomatic individuals. In a meta-analysis evaluating 9592 patients, CCTA demonstrated a graded increase in adverse events following CCTA performance for no CAD, nonobstructive CAD, and obstructive CAD (any vessel with greater than 50% luminal stenosis).[17] Particularly for individuals without known CAD, the pooled annualized event rate was low compared with that of obstructive CAD (0.17% vs 8.8%).[17] CCTA also demonstrated a good prognostic value in various groups, such as young patients with a family history of CAD[18] and ethnic groups.[19] Combining CAD data with measures of left ventricular (LV) function provides incremental prognostic utility, with LV ejection fractions less than 50%, conferring a worsened prognosis. Perhaps most importantly, a normal finding on CCTA was associated with a very low annual mortality rate of 0.13%.[20]

Current-generation CCTA is nevertheless not without limitations. Although anatomical assessment by CCTA is diagnostically sound with a robust ability to predict prognosis,[11,14,20,21] CCTA measurements of stenoses do not accurately predict their functional significance.[22] Furthermore, usage of iodinated contrast material and exposure to radiation are also important considerations. Pertaining to the latter, numerous radiation dose–reduction methods have been introduced and now enable CCTA performance at levels similar to that of background radiation exposure from radon.

The near-term future of CCTA holds promise for better detection of coronary artery lesions. One such effort to overcome certain limitations of current-generation CCTA is in dual-energy CT, which exhibits improved image quality by a reduction in noise without additional radiation dose than that with single-energy CT.[23] When compared with ICA images, dual-energy CT showed 90% sensitivity, 94% specificity, and 93% accuracy for the detection of greater than 50% luminal stenosis.[24] Certain CT acquisition systems also demonstrate increased temporal resolution than single-energy CT does,[25] an attribute that obviates the need for heart rate control in all individuals and may improve the ability of CT to evaluate the severity of lesion stenosis, particularly in patients who do not achieve adequate heart rate control during the examination.

Cardiac CTP

Recent advances in technology allow for assessment of myocardial perfusion by CT. Multidetector CT systems can image in a dynamic mode, in which sequential images are obtained over a period to record the kinetics of iodinated contrast in the arterial blood pool and the myocardium.[26] George et al,[26] using a 64-detector CT in a canine ischemia model, performed CTP during adenosine infusion. They found strong correlations between the ratio of myocardial to LV upslope and microsphere-derived myocardial blood flow (MBF). The authors replicated the study in humans with adenosine stress 64- and 256-row detector CCTA and CTP (Fig. 1). In the human study, they calculated transmural perfusion ratio (subendocardial attenuation-subepicardial attenuation), which had a significant inverse linear correlation ($r = 0.63$, $P = 0.001$) with percentage diameter stenosis on quantitative ICA. Furthermore, the combination of CTP and CCTA was 86% sensitive and 92% specific for identifying patients with atherosclerosis causing perfusion abnormalities when compared with that of the combination of ICA and SPECT-MPI as the gold standard.[27] In a prospective multi-center international trial, the combined coronary atherosclerosis and myocardial perfusion evaluation using 320-detector row CT (CORE320) trial evaluated CT for the identification of CAD (≥50% luminal stenosis) and corresponding myocardial perfusion defect in patients with suspected CAD. This method demonstrated a utility of CTP in patients with chest pain, as CCTA with concomitant CTP was as effective as sequential SPECT-MPI and invasive angiography for identifying flow-limiting atherosclerotic lesions.[28] In 381 patients from 16 centers, the patient-based diagnostic accuracy defined by AUC of integrated CTA-CTP for detecting or excluding flow-limiting CAD was 0.87 (95% CI: 0.84-0.91). It showed better accuracy in patients without prior myocardial infarction (MI) (AUC = 0.90) and without prior CAD (AUC = 0.93).[29]

Given the nascent stage for CTP, data regarding the prognostic utility of CTP deficits remain unknown and require evaluation in prospective multicenter efforts. Furthermore, the cost and the clinical effectiveness need to be examined, with a particular focus on safety because of additional ionizing radiation exposure. Continuing development of CT technology may ameliorate some of these concerns, with new acquisition protocols such as using prospective electrocardiogram-gated scans .[30]

Fractional Flow Reserve Derived From CT (FFR_{CT})

At present, the "gold"-standard assessment of the hemodynamic significance of coronary stenosis is FFR.[31] Recent advances in computational fluid dynamics now enable the calculation of coronary flow and pressure fields from anatomical image data (Fig. 2).[32] Applied to CT, these technologies enable calculation of FFR, which is defined as the ratio of maximal MBF through a diseased artery to the blood flow in the hypothetical case in which the artery was normal. Several studies have demonstrated an incremental value of FFR_{CT} for the diagnosis of hemodynamically significant CAD. In the diagnosis of ischemia-causing stenoses obtained via noninvasive fractional flow reserve (DISCOVER-FLOW) trial, when compared with invasive FFR, noninvasive FFR_{CT} demonstrated a per-vessel accuracy, sensitivity, specificity, PPV, and NPV for lesions causing ischemia of 84.3%, 87.9%, 82.2%, 73.9%, and 92.2%, respectively.[33] The performance of FFR_{CT} was superior to CT stenosis for diagnosing ischemic lesions; the latter of which demonstrated an accuracy, sensitivity, specificity, PPV, and NPV of 58.5%, 91.4%, 39.6%, 46.5%, and 88.9%, respectively. The determination of fractional flow reserve by anatomic computed tomographic angiography (DeFACTO) trial—a multicenter international study evaluating FFR_{CT} against CT for diagnostic accuracy of ischemia[34]— consisted of 252 patients in whom 407 vessels were directly interrogated by invasive FFR. On a per-patient basis, FFR_{CT} was superior to CT stenosis for diagnosis of ischemic lesions for accuracy (73% vs 64%), sensitivity (90% vs 84%), specificity (54% vs 42%), PPV (67% vs 61%), and NPV (84% vs 72%). The AUC of FFR_{CT} also showed improved discrimination over CT stenosis alone (0.68 [95% CI: 0.62-0.74] vs 0.81 [0.75-0.86]; $P < 0.001$). In patients with intermediate stenosis (30%-69%), there was more than a 2-fold increase in sensitivity, from 37%-82%, with no loss of specificity.[35] Evaluation of stenosis by FFR_{CT} also demonstrated superior discrimination when compared with that by CCTA based on per-patient and per-vessel analysis in patients with intermediate CAD. In a subsequent study of 96 patients, the use of FFR_{CT} to select patients for ICA and percutaneous coronary intervention (PCI) resulted in 30% lower costs and 12% fewer events at 1 year when compared with that in the most commonly used ICA or visual strategy.[36] Most recently, the HeartFlowNXT study showed a more accurate determination of which arterial blockages are associated with coronary ischemia than that shown by standard CCTA or by ICA.[37] In this prospective, international study that enrolled 254 patients scheduled to undergo nonemergent clinically indicated ICA owing to suspected CAD, FFR_{CT} data matched closely with invasively measured FFR. The AUC for FFR_{CT} (≤0.80) was 0.82 vs 0.63 for CCTA (≤0 stenosis) ($P < 0.0001$) with invasive FFR as the reference standard. The per-patient sensitivity and specificity were 86% and 79% for FFR_{CT} vs 94% and 34% for CCTA, and 91% and 51% for ICA (>50% luminal stenosis), respectively.

Recently, FFR_{CT} demonstrated its value on not only diagnostic area but also therapeutic prediction modeling. In a study conducted in 44 patients, FFR_{CT} was shown to be feasible for predicting the functional outcome of PCI by virtual stenting models, that is, prediction of ischemia reduction. Diagnostic accuracy of FFR_{CT} to predict ischemia (FFR ≥ 0.8) after stenting was 96% (sensitivity = 100%, specificity = 96%, PPV = 50%, and NPV = 100%). This study showed that virtual coronary stenting of CT-derived computational models is feasible and that this novel noninvasive technology may be useful in predicting functional

outcomes after coronary stenting.[38] Further studies are needed to elucidate the role of FFR_{CT} figures in the evaluation of in-stent restenosis, coronary artery bypass grafts, and prognosis.

FFR_{CT} offers several practical advantages in that it does not require modification of CT angiography protocols, does not require administration of additional medications beyond what is typically administered for CCTA, and does not result in any additional radiation exposure. However, certain artifacts may affect CT interpretability, including coronary motion. Additional limitations of FFR_{CT} relate to assumptions in the physiological models that include population as well as patient-specific data. Relationships relating myocardial mass to total coronary flow, the relative coronary microvascular resistance based on vessel size, or reductions in resistance in response to adenosine-mediated hyperemia vary amongst patients. In patients with microvascular disease, models of adenosine-mediated hyperemia may overestimate the degree of vasodilation, resulting in FFR_{CT} values that are less than those of measured FFR.

MPI by SPECT and PET

SPECT is a robust imaging modality that has been widely used in clinical practice and its diagnostic accuracy, value in risk assessment, and prognosis are well established. A meta-analysis of 79 SPECT studies, including 8964 patients, demonstrated average sensitivities and specificities of 86% and 74%, respectively.[39] A more recent meta-analysis of 117 SPECT studies revealed a sensitivity of 88.3% and specificity of 75.8%.[40] Patients with abnormal myocardial perfusion SPECT (MPS) have on average an annual event rate (cardiac death or MI) of 6.7%.[39] By contrast, a normal MPS confers generally good clinical outcomes. A total of 16 studies performed between 1994 and 2001, which reported 20,983 patients with normal MPS and a mean follow-up of 28 months, observed a rate of death due to cardiac disease or MI of 0.7% per year, a rate similar to that of an asymptomatic population.[41] Similar findings have recently been reported in a multi-center registry of 4728 patients. The observed annualized survival rate for those patients with a normal finding on ^{99m}Tc-tetrofosmin evaluation was 0.6%. Similarly, excellent survival rates were noted for the male and female subsets of this population as well as for patients who could exercise and for those undergoing pharmacologic stress testing.[42] Accuracy of SPECT may improve in the setting of newer imaging equipment, radiotracers, image acquisition, and reconstruction techniques. The recently introduced camera systems with optimized acquisition geometry, collimator design, and reconstruction software have the potential to improve image quality with significantly shorter image acquisition times and reduced isotope doses, but whether these technological advances translate to improved clinical performance remains to be definitively addressed.[43]

The incremental value of hybrid cardiac imaging with SPECT and CT has also been of interest. In the first report of 38 patients with perfusion defects on SPECT, the number of lesions with equivocal hemodynamic relevance was significantly reduced using SPECT/CT fusion when compared with that using side-by-side analysis.[44] This added clinical value was observed in 29% of patients and was particularly common in patients with multivessel disease and intermediate severity stenosis or in patients with diseases side branches. A study

implementing motion-frozen SPECT data and CT-guided SPECT contour and territory adjustments found that the improved diagnostic value of hybrid imaging was mainly driven by higher diagnostic indices in left circumflex and right coronary artery territories.[45] In a study including more than 500 patients with a normal SPECT study who also underwent concomitant CCTA, patients an abnormal CCTA was associated with a higher rate the combined end point.[46]

The following 2 new high-efficiency cardiac cameras have been introduced: Discovery NM 530c (GE Healthcare, Israel) and D-SPECT (Spectrum Dynamics, Israel), and they are based on an array of cadmium-zinc-telluride (CZT)–pixilated detectors. The use of CZT detectors has advantages of superior energy resolution and spatial resolution while acquiring 19 cardiac views.[47] CZT SPECT imaging demonstrated 95% sensitivity and 69% accuracy for detecting obstructive CAD by ICA defined as ≥70% narrowing.[48] In a study of consecutive patients without known CAD, patients undergoing CZT SPECT required a lower mean total administered isotope dose per patient and shorter imaging time than the ones undergoing the hybrid SPECT/64-slice CT.[49,50]

PET has also demonstrated high diagnostic performance for the diagnosis of CAD. A study comparing the diagnostic accuracy between PET and SPECT observed the image quality to be excellent in 78% of PET studies when compared with that in 62% of SPECT studies, a finding that was associated with higher accuracy with PET (89% vs 79%). The superiority of PET was maintained in patients who were obese, a problematic population for SPECT.[51] The superior quality and accuracy of PET have been attributed to its better spatial resolution and attenuation correction, an advantage that is particularly relevant in patients prone to soft tissue attenuation artifacts. A meta-analysis[52] of 114 SPECT studies (13,741 patients) and 15 PET studies (1319 patients) demonstrated average sensitivities and specificities of 88% and 61% for SPECT and 84% and 81% for PET, respectively. Another meta-analysis demonstrated that[53] PET MPI using rubidium-82 (^{82}Rb) possesses superior sensitivity and specificity than that of SPECT for the detection of CAD. This study showed sensitivities of 85% (CI: 0.82-0.87) and 90% (CI: 0.88-0.92) and specificities of 85% (CI: 0.82-0.87) and 88% (CI: 0.85-0.91) for SPECT and PET, respectively. Summary of receiver operating characteristic curves was computed: AUC was 0.90 and 0.95 for SPECT and PET, respectively ($P < 0.0001$).

PET MPI is also employed for evaluating intramyocardial microvascular function through the measurement of absolute MBF at rest and at peak stress (Fig. 3). With dynamic perfusion images, image-derived time-activity curves from the arterial blood and myocardial tissue regions are used as inputs to a tracer kinetic model. The rate of uptake of the tracer into the myocardial tissue provides an estimate of MBF on an absolute scale of mL/min/g. This technique also allows the calculation of the myocardial flow reserve (MFR), which is the ratio of MBF at peak hyperemia to resting MBF.[54,55] MBF and MFR demonstrated prognostic value as an additional marker for adverse cardiac events.[56-59] Herzog et al[56] demonstrated that in the setting of a normal MPI result, a preserved CFR-MFR of more than 2.0 is a strong predictor of a good event-free survival through 3 years with an adverse prognosis seen in the setting of a reduced MFR. In addition, MFR results have been

observed to effectively stratify patients based on their risk of adverse cardiovascular events in those with normal and those with abnormal stress perfusion.

Recently, integrated PET/CT has been demonstrated to offer accurate spatial coregistration of myocardial perfusion defects and subtending coronary arteries (Fig. 4). In a recent study, Javadi et al[61] compared standardized myocardial vascular territories with individual coregistered myocardial territories using ^{82}Rb PET/CT and found disagreement in 9% of the segments. Notably, in 72% of patients, a disagreement in at least one myocardial segment was found. Most frequently, standard right coronary segments were reassigned to the left circumflex artery territory (39% of reassigned segments), and standard circumflex segments were reassigned to the left anterior descending territory (30%). The PET/CT images allowed for identi-fication of flow-limiting coronary lesions that required a revascularization procedure (as defined by ICA and PET) with a sensitivity, specificity, PPV, and NPV of 90%, 98%, 82%, and 99%, respectively. These results were confirmed by a similar study with SPECT/CT that demonstrated the hybrid approach to result in a significant improvement in specificity (from 63%-95%) and PPV (from 31%-77%) when compared with that by CCTA alone for detecting flow-limiting coronary stenosis.[62] A similar diagnostic performance was reported by Groves et al. using a ^{82}Rb PET/CT hybrid system.[63] Notably, most nonevaluable severely calcified vessels in the left anterior descending artery had positive findings on stress nuclear MPI, whereas most nonevaluable vessels with motion artifacts in the right coronary artery had negative findings.

Some studies have described the development of “normal databases” characterizing relative perfusion data for patients with a low likelihood of CAD.[64,65] These databases objectively define the normal range of relative perfusion values to evaluate patients with suspected CAD and determine whether the perfusion distribution is normal or abnormal. These databases can be used as an adjunct to the subjective visual scan interpretation by the clinician. Most of the previous studies that have developed low likelihood normal databases have done so only in the context of SPECT or 2D PET MPI. Recently, 3-dimensional (3D) ^{82}Rb PET normal database containing the relative perfusion scores of patients without obstructive CAD demonstrated a good diagnostic value. Its normalcy rate was 95%. Sensitivity was 100% for detecting patients with either 50% or 70% stenosis. Optimal specificity was 87% for either 50% or 70% stenosis.[65]

PET also enables assessment of myocardial viability and hibernation. In a recent meta-analysis (24 studies, 756 patients), the sensitivity and specificity values of PET were 92% and 63%, respectively.[66] Regarding recovery of LV function after revascularization, PET demonstrated a higher sensitivity but comparable specificity to all imaging techniques.[66] In another meta-analysis that included more recent studies from 1998-2006, patients with ischemic LV dysfunction (LV ejection fraction ≤45%) were more sensitively examined by PET, albeit at a cost of specificity when compared with nonnuclear techniques to predict recovery of global LV dysfunction.[67] However, the risk of death after revascularization was similar unless the extent of viable tissue was more than 20% of LV.[68]

Although PET has shown its usefulness in clinical assessment of myocardial perfusion and viability, there are several limitations, such as limited availability, methodological

complexity, and high costs. Nonnegligible radiation doses are associated with PET, but current PET perfusion stress-rest imaging (including absolute quantification of myocardial perfusion) can be performed with much lower doses (<4 mSv) when compared with that for SPECT, particularly with the use of new 3D PET/CT scanners.[69,70] Furthermore, absolute quantification of myocardial perfusion has several limitations that need to be recognized. The optimal cutoff values for absolute perfusion need to be defined in large populations and for various tracers, and potential sources of errors in mean flow rate measurements from PET-based perfusion imaging need to be remembered, including the effect of high coronary driving pressures and resting flow rates. In addition, a further study is required as to how MFR may effectively differentiate between patients who have epicardial stenosis and patients who have abnormalities with subendocardial microvascular perfusion. Furthermore, additional information is needed to address important subpopulations such as patients who are diabetic and obese, patients with heart failure, and patients who have undergone revascularization.

Cardiac MRI

Perfusion CMR studies employ the use of “first pass” of an intravenously injected gadolinium contrast agent during vasodilator (ie, adenosine or dipyridamole) challenge to identify hemodynamically significant coronary artery stenosis. At present, this technique has been well validated, showing similar or better diagnostic accuracies than routinely used techniques, such as SPECT[71-73] or stress echocardiography, did.[74] The MRI for myocardial perfusion assessment in CAD trial[73] was a multicenter, multivendor prospective trial, which compared perfusion CMR with SPECT for the detection of ischemia, with quantitative coronary angiography as the gold standard. It was reported that perfusion CMR in the entire study population was superior to SPECT. Nagel et al[74] compared dobutamine stress CMR (DSMR) with dobutamine stress echocardiography (DSE) in the detection of CAD (≥50% stenosis) using ICA as the gold standard. They reported that DSMR has a higher diagnostic accuracy than that of DSE in patients with suspected CAD. The sensitivity increased from 74%-86% and specificity increased from 69.8%-85.7% (both $P < 0.05$) for DSE and DSMR, respectively. A meta-analysis of DSMR using 14 data sets demonstrated a sensitivity of 83% and a specificity of 86% on a per-patient level.[75] These studies included patients who were selected to undergo catheterization and had a relatively high disease prevalence of 71%. Perfusion of the myocardium can be assessed qualitatively or quantitatively by calculating the myocardial perfusion reserve index (MPRI).[76] To calculate MPRI, the relative upslope of the signal intensity of a given segment during stress is divided by the relative upslope of the same segment at rest. The MPRI has been validated during ICA, and an MPRI of 1.5[77] or 2.0[78] correlated with FFR measurements of ≤0.75 or with ≥50% luminal stenosis. In a prospective study, perfusion CMR was compared with PET and quantitative coronary angiography in detection and sizing of compromised myocardium in 48 patients and 18 healthy subjects.[79] This study observed that a perfusion CMR approach reliably identifies patients with coronary artery stenosis and provides information on the amount of compromised myocardium. Furthermore, an array of studies showed that ischemia by stress perfusion CMR and DSMR is an independent predictor of cardiac events.[80] Normal stress perfusion CMR or DSMR predicted a 3-year event-free survival of 99.2%. This concept has been further validated for stress perfusion CMR, where strong prognostic values were

demonstrated for both male and female patients,[81] and also for DSMR, in which test results were highly predictive of cardiac events in 1369 patients who were followed up for 4 years.[82] The advantage of stress perfusion CMR over modalities such as SPECT is the ability to distinguish between subendocardial and transmural perfusion defects.

A potential limitation of CMR stress imaging is that current pulse sequences often demonstrate a “dark-rim” artifact that can be mistaken for a true perfusion abnormality.[83] This artifact is explained by a multitude of factors, such as a motion during data acquisition, Gibbs ringing caused by resolution limitations, or susceptibility artifacts from the passage of the contrast agents.[84-86] Recent technology such as higher spatial resolution CMR might reduce this artifact. However, more data are needed to define the optimal application of this technique on CMR perfusion.[87]

Delayed-Enhancement MRI

Patients with ischemic cardiomyopathy may be more likely to benefit from revascularization if viable tissue is present. Direct imaging of myocardial fibrosis is possible with the use of an inversion recovery–prepared T1-weighted gradient echo sequence after the intravenous administration of gadolinium. This CMR technique has been named delayed-enhancement MRI (DE-MRI) and demonstrates nonviable tissue as hyper-enhanced or bright. The clinical utility of DE-MRI in the delineation of nonviable myocardium has been confirmed by direct comparison with several clinically established markers of myocardial viability, including contractile reserve, perfusion, metabolism, and, most recently, electromechanical mapping.[88] The performance of DE-MRI for the detection of MI was tested in an international, multicenter, randomized trial.[89] In total, 282 patients with acute and 284 with chronic first-time MI were scanned in 26 centers. The study showed that the sensitivity of DE-MRI increased with increasing gadolinium dose, reaching 99% and 94% in acute and chronic MI, respectively, with the 0.3-mmol/kg dose. Furthermore, with doses 0.2 mmol/kg or higher, when MI was identified, it was in the correct location in more than 97% of patients.[89] However, optimal dose of gadolinium contrast might be challenging, as it needs to be balanced between higher dose for better image quality[89] and limitations such as the cost, brighter blood pools that may obscure subendocardial infarcts,[90] and an increased concern for nephrogenic systemic fibrosis in patients with severe renal impairment.[91] Furthermore, to date, although DE-MRI has been demonstrated to be a robust prognostic tool, its use to guide revascularization strategies has not been observed.

MR Coronary Angiography

Tremendous advances in MRI technique during the past decade have demonstrated potential for noninvasive diagnosis of CAD. The image resolution of current coronary artery MR techniques is approximately 1 mm, which is sufficient for the detection of stenosis in large coronary arteries but likely inadequate for accurate detection of disease in smaller branches of the coronary vasculature. A multicenter study from Japan was reported for 138 patients using a whole-heart MR coronary imaging technique. The acquisition of images was successfully completed in 92% of patients. The sensitivity of MR coronary angiography was 88% and the specificity was 72% for CAD detection (≥50% luminal stenosis by ICA).[92] However, a significant limitation of MR coronary angiography is that test performance with

contemporary technology (1.5 T, 3D navigator echo) can vary significantly with operator experience. The potential magnitude of this effect was illustrated in a study in which a 1.5-T MRI scanner was used in 21 patients; all images from 2 patients and 4 coronary segments from the remaining 19 patients were excluded from analysis because of poor image quality.[93] The remaining 186 proximal, middle, or distal coronary segments were interpreted by 2 observers. For the prediction of ≥50% stenosis by the 2 observers, sensitivity was 44% and 56% and the specificity was 95% and 84%. A meta-analysis of 51 studies compared the diagnostic performance of CCTA and MR coronary angiography for the detection of ≥50% diameter stenosis.[94] CCTA had significantly higher sensitivity (85% vs 72% with CMR) and specificity (95% vs 87%). A distinct meta-analysis by Schuetz et al[95] yielded a mean sensitivity and specificity of 97.2% and 87.4% for CCTA and 87.1% and 70.3% for MR coronary angiography, respectively. For ruling out CAD, CCTA is more accurate than MR coronary angiography, when scanners with more than 16 rows improve sensitivity, as do slowed heart rates.

Plaque Assessment Using CMR

CMR has shown potential for atherosclerotic plaque assessment.[96] Hyperintensity plaque in T1-weighted imaging was related with positive remodeling, ultrasound attenuation, lower Hounsfield units, and transient slow flow after PCI, which are related to vulnerable plaques.[10,96,97] Hyperintensity plaque also related with presence of intracoronary thrombus detected by optical coherence tomography in patients with angina.[98] Accordingly, the future role of coronary MRI may be as an important adjunct to the comprehensive CMR examination, which combines anatomical, functional, and plaque assessment. Direct correlation of MR angiographic abnormalities with perfusion and wall motion abnormalities may also prove to be a powerful combination in the evaluation of CAD.

Conclusion

An array of high-quality imaging technologies exist to study individuals with suspected CAD, with benefits and limitations to each of them. Selection of the best test depends on the patient risk factors and the local availability and expertise of each modality. This integrated approach combining anatomical and functional imaging is critical for comprehensive evaluation of the clinically relevant aspects of CAD.

Supplementary Material

Refer to Web version on PubMed Central for supplementary material.

Acknowledgments

This study was funded by grants from the National Institutes of Health, USA (R01HL115150 and R01HL118019), as well as generous gifts from the Dalio Foundation and the Michael J. Wolk Foundation.

References

1. Murray CJL, Lopez AD. Alternative projections of mortality and disability by cause 1990-2020: Global Burden of Disease study. Lancet. 1997; 349:1498–1504. [PubMed: 9167458]

2. Roger VL, Go AS, Lloyd-Jones DM, et al. Heart disease and stroke statistics —2011 Update: A report from the American Heart Association. Circulation. 2011; 123:e18–e209. [PubMed: 21160056]

3. Who. World Health Statistics. World Health Organization; 2008. 2008

4. Budoff MJ, Dowe D, Jollis JG, et al. Diagnostic performance of 64-multidetector row coronary computed tomographic angiography for evaluation of coronary artery stenosis in individuals without known coronary artery diseaseresults from the prospective multicenter ACCURACY (assessment by coronary computed tomographic angiography of individuals undergoing invasive coronary angiography) Trial. J Am Coll Cardiol. 2008; 52:1724–1732. [PubMed: 19007693]

5. Miller JM, Rochitte CE, Dewey M, et al. Diagnostic performance of coronary angiography by 64-row CT. N Engl J Med. 2008; 359:2324–2336. [PubMed: 19038879]

6. Meijboom WB, Meijs MF, Schuijf JD, et al. Diagnostic accuracy of 64-slice computed tomography coronary angiography: A prospective, multi-center, multivendor study. J Am Coll Cardiol. 2008; 52:2135–2144. [PubMed: 19095130]

7. Stein PD, Yaekoub AY, Matta F, et al. 64-Slice CT for diagnosis of coronary artery disease: A systematic review. Am J Med. 2008; 121:715–725. [PubMed: 18691486]

8. Bluemke DA, Achenbach S, Budoff M, et al. Noninvasive coronary artery imaging: Magnetic resonance angiography and multidetector computed tomography angiography: A scientific statement from the American Heart Association Committee on Cardiovascular Imaging and Intervention of the Council on Cardiovascular Radiology and Intervention, and the Councils on Clinical Cardiology and Cardiovascular Disease in the Young. Circulation. 2008; 118:586–606. [PubMed: 18586979]

9. Schroeder S, Achenbach S, Bengel F, et al. Cardiac computed tomography: Indications, applications, limitations, and training requirements: Report of a Writing Group deployed by the Working Group Nuclear Cardiology and Cardiac CT of the European Society of Cardiology and the European Council of Nuclear Cardiology. Eur Heart J. 2008; 29:531–556. [PubMed: 18084017]

10. Motoyama S, Kondo T, Sarai M, et al. Multislice computed tomographic characteristics of coronary lesions in acute coronary syndromes. J Am Coll Cardiol. 2007; 50:319–326. [PubMed: 17659199]

11. Min JK, Shaw LJ, Devereux RB, et al. Prognostic value of multidetector coronary computed tomographic angiography for prediction of all-cause mortality. J Am Coll Cardiol. 2007; 50:1161–1170. [PubMed: 17868808]

12. Nakazato R, Shalev A, Doh JH, et al. Quantification and characterisation of coronary artery plaque volume and adverse plaque features by coronary computed tomographic angiography: A direct comparison to intravascular ultrasound. Eur Radiol. 2013; 23:2109–2117. [PubMed: 23553587]

13. Nakazato R, Shalev A, Doh JH, et al. Aggregate plaque volume by coronary computed tomography angiography is superior and incremental to luminal narrowing for diagnosis of ischemic lesions of intermediate stenosis severity. J Am Coll Cardiol. 2013; 62:460–467. [PubMed: 23727206]

14. Lin FY, Shaw LJ, Dunning AM, et al. Mortality risk in symptomatic patients with nonobstructive coronary artery disease: A prospective 2-center study of 2,583 patients undergoing 64-detector row coronary computed tomographic angiography. J Am Coll Cardiol. 2011; 58:510–519. [PubMed: 21777749]

15. Fischer C, Hulten E, Belur P, et al. Coronary CT angiography versus intravascular ultrasound for estimation of coronary stenosis and athero-sclerotic plaque burden: A meta-analysis. J Cardiovasc Comput Tomogr. 2013; 7:256–266. [PubMed: 24148779]

16. de Graaf MA, Broersen A, Kitslaar PH, et al. Automatic quantification and characterization of coronary atherosclerosis with computed tomography coronary angiography: Cross-correlation with intravascular ultrasound virtual histology. Int J Cardiovasc Imaging. 2013; 29:1177–1190. [PubMed: 23417447]

17. Hulten EA, Carbonaro S, Petrillo SP, et al. Prognostic value of cardiac computed tomography angiography: A systematic review and meta-analysis. J Am Coll Cardiol. 2011; 57:1237–1247. [PubMed: 21145688]

18. Otaki Y, Gransar H, Berman DS, et al. Impact of family history of coronary artery disease in young individuals (from the CONFIRM registry). Am J Cardiol. 2013; 111:1081–1086. [PubMed: 23411105]
19. Hulten E, Villines TC, Cheezum MK, et al. Usefulness of coronary computed tomography angiography to predict mortality and myocardial infarction among Caucasian, African and East Asian ethnicities (from the CONFIRM [Coronary CT Angiography Evaluation for Clinical Outcomes: An International Multicenter] Registry). Am J Cardiol. 2013; 111:479–485. [PubMed: 23211358]
20. Chow BJ, Small G, Yam Y, et al. Incremental prognostic value of cardiac computed tomography in coronary artery disease using CONFIRM: COroNary computed tomography angiography evaluation for clinical outcomes: An InteRnational Multicenter registry. Circ Cardiovasc Imaging. 2011; 4:463–472. [PubMed: 21730027]
21. Chow BJ, Wells GA, Chen L, et al. Prognostic value of 64-slice cardiac computed tomography severity of coronary artery disease, coronary atherosclerosis, and left ventricular ejection fraction. J Am Coll Cardiol. 2010; 55:1017–1028. [PubMed: 20202518]
22. Meijboom WB, Van Mieghem CAG, van Pelt N, et al. Comprehensive assessment of coronary artery stenoses. J Am Coll Cardiol. 2008; 52:636–643. [PubMed: 18702967]
23. Halliburton SS, Sola S, Kuzmiak SA, et al. Effect of dual-source cardiac computed tomography on patient radiation dose in a clinical setting: Comparison to single-source imaging. J Cardiovasc Comput Tomogr. 2008; 2:392–400. [PubMed: 19083984]
24. Ruzsics B, Schwarz F, Schoepf UJ, et al. Comparison of dual-energy computed tomography of the heart with single photon emission computed tomography for assessment of coronary artery stenosis and of the myocardial blood supply. Am J Cardiol. 2009; 104:318–326. [PubMed: 19616661]
25. Achenbach S, Ropers U, Kuettner A, et al. Randomized comparison of 64-slice single- and dual-source computed tomography coronary angiography for the detection of coronary artery disease. JACC Cardiovasc Imaging. 2008; 1:177–186. [PubMed: 19356426]
26. George RT, Jerosch-Herold M, Silva C, et al. Quantification of myocardial perfusion using dynamic 64-detector computed tomography. Invest Radiol. 2007; 42:815–822. [PubMed: 18007153]
27. George RT, Arbab-Zadeh A, Miller JM, et al. Adenosine stress 64- and 256-row detector computed tomography angiography and perfusion imaging: A pilot study evaluating the transmural extent of perfusion abnormalities to predict atherosclerosis causing myocardial ischemia. Circ Cardiovasc Imaging. 2009; 2:174–182. [PubMed: 19808590]
28. Vavere AL, Simon GG, George RT, et al. Diagnostic performance of combined noninvasive coronary angiography and myocardial perfusion imaging using 320 row detector computed tomography: Design and implementation of the CORE320 multicenter, multinational diagnostic study. J Cardiovasc Comput Tomogr. 2011; 5:370–381. [PubMed: 22146496]
29. Rochitte CE, George RT, Chen MY, et al. Computed tomography angiography and perfusion to assess coronary artery stenosis causing perfusion defects by single photon emission computed tomography: The CORE320 study. Eur Heart J. 2013
30. Becker A, Becker C. CT imaging of myocardial perfusion: Possibilities and perspectives. J Nucl Cardiol. 2013; 20:289–296. [PubMed: 23479267]
31. Pijls NHJ, de Bruyne B, Peels K, et al. Measurement of fractional flow reserve to assess the functional severity of coronary-artery stenoses. N Engl J Med. 1996; 334:1703–1708. [PubMed: 8637515]
32. Taylor CA, Fonte TA, Min JK. Computational fluid dynamics applied to cardiac computed tomography for noninvasive quantification of fractional flow reserve: Scientific basis. J Am Coll Cardiol. 2013; 61:2233–2241. [PubMed: 23562923]
33. Koo BK, Erglis A, Doh JH, et al. Diagnosis of ischemia-causing coronary stenoses by noninvasive fractional flow reserve computed from coronary computed tomographic angiograms. Results from the prospective multi-center DISCOVER-FLOW (diagnosis of ischemia-causing stenoses obtained via noninvasive fractional flow reserve) study. J Am Coll Cardiol. 2011; 58:1989–1997. [PubMed: 22032711]

34. Min JK, Leipsic J, Pencina MJ, et al. Diagnostic accuracy of fractional flow reserve from anatomic CT angiography. J Am Med Assoc. 2012; 308:1237–1245.
35. Nakazato R, Park H-B, Berman DS, et al. Noninvasive fractional flow reserve derived from computed tomography angiography for coronary lesions of intermediate stenosis severity results from the DeFACTO study. Circ Cardiovasc Imaging. 2013; 6:881–889. [PubMed: 24081777]
36. Hlatky MA, Saxena A, Koo BK, et al. Projected costs and consequences of computed tomography-determined fractional flow reserve. Clin Cardiol. 2013
37. Norgaard BL, Leipsic J, Gaur S, et al. Diagnostic performance of noninvasive fractional flow reserve derived from coronary CT angiography in suspected coronary artery disease: The NXT trial. J Am Coll Cardiol. 2014
38. Kim K-H, Doh J-H, Koo B-K, et al. A novel noninvasive technology for treatment planning using virtual coronary stenting and computed tomography-derived computed fractional flow reserve. JACC Cardiovasc Interv. 2013; 7:72–78. [PubMed: 24332418]
39. Underwood SR, Anagnostopoulos C, Cerqueira M, et al. Myocardial perfusion scintigraphy: The evidence. Eur J Nucl Med Mol Imaging. 2004; 31:261–291. [PubMed: 15129710]
40. Parker MW, Iskandar A, Limone B, et al. Diagnostic accuracy of cardiac positron emission tomography versus single photon emission computed tomography for coronary artery disease. Clinical perspective: A bivariate meta-analysis. Circ Cardiovasc Imaging. 2012; 5:700–707. [PubMed: 23051888]
41. Russell RO Jr, Sutton MGSJ, Udelson JE, et al. ACC/AHA/ASNC guidelines for the clinical use of cardiac radionuclide imaging. J Am Coll Cardiol. 2003
42. Shaw LJ, Hendel R, Borges-Neto S, et al. Prognostic value of normal exercise and adenosine ^{99m}Tc-tetrofosmin SPECT imaging: Results from the multicenter registry of 4,728 patients. J Nucl Med. 2003; 44:134–139. [PubMed: 12571200]
43. Garcia EV, Faber TL, Esteves FP. Cardiac dedicated ultrafast SPECT cameras: New designs and clinical implications. J Nucl Med. 2011; 52:210–217. [PubMed: 21233190]
44. Gaemperli O, Schepis T, Valenta I, et al. Cardiac image fusion from stand-alone SPECT and CT: Clinical experience. J Nucl Med. 2007; 48:696–703. [PubMed: 17475956]
45. Slomka PJ, Cheng VY, Dey D, et al. Quantitative analysis of myocardial perfusion SPECT anatomically guided by coregistered 64-slice coronary CT angiography. J Nucl Med. 2009; 50:1621–1630. [PubMed: 19759104]
46. van Werkhoven JM, Schuijf JD, Gaemperli O, et al. Prognostic value of multislice computed tomography and gated single-photon emission computed tomography in patients with suspected coronary artery disease. J Am Coll Cardiol. 2009; 53:623–632. [PubMed: 19215839]
47. Slomka PJ, Patton JA, Berman DS, et al. Advances in technical aspects of myocardial perfusion SPECT imaging. J Nucl Cardiol. 2009; 16:255–276. [PubMed: 19242769]
48. Duvall WL, Sweeny JM, Croft LB, et al. Comparison of high efficiency CZT SPECT MPI to coronary angiography. J Nucl Cardiol. 2011; 18:595–604. [PubMed: 21638154]
49. Mouden M, Timmer JR, Ottervanger JP, et al. Impact of a new ultrafast CZT SPECT camera for myocardial perfusion imaging: Fewer equivocal results and lower radiation dose. Eur J Nucl Med Mol Imaging. 2012; 39:1048–1055. [PubMed: 22426827]
50. Nakazato R, Tamarappoo BK, Kang X, et al. Quantitative upright-supine high-speed SPECT myocardial perfusion imaging for detection of coronary artery disease: Correlation with invasive coronary angiography. J Nucl Med. 2010; 51:1724–1731. [PubMed: 20956478]
51. Bateman TM, Heller GV, McGhie AI, et al. Diagnostic accuracy of rest/ stress ECG-gated Rb-82 myocardial perfusion PET: Comparison with ECG-gated Tc-99 m sestamibi SPECT. J Nucl Cardiol. 2006; 13:24–33. [PubMed: 16464714]
52. Jaarsma C, Leiner T, Bekkers SC, et al. Diagnostic performance of noninvasive myocardial perfusion imaging using single-photon emission computed tomography, cardiac magnetic resonance, and positron emission tomography imaging for the detection of obstructive coronary artery disease: A meta-analysis. J Am Coll Cardiol. 2012; 59:1719–1728. [PubMed: 22554604]
53. Mc Ardle BA, Dowsley TF, deKemp RA, et al. Does rubidium-82 PET have superior accuracy to SPECT perfusion imaging for the diagnosis of obstructive coronary disease?: A systematic review and meta-analysis. J Am Coll Cardiol. 2012; 60:1828–1837. [PubMed: 23040573]

54. Di Carli MF, Murthy VL. Cardiac PET/CT for the evaluation of known or suspected coronary artery disease. Radiographics. 2011; 31:1239–1254. [PubMed: 21918042]
55. Klein R, Beanlands RS, deKemp RA. Quantification of myocardial blood flow and flow reserve: Technical aspects. J Nucl Cardiol. 2010; 17:555–570. [PubMed: 20596841]
56. Herzog BA, Husmann L, Valenta I, et al. Long-term prognostic value of ^{13}N-ammonia myocardial perfusion positron emission tomo graphy added value of coronary flow reserve. J Am Coll Cardiol. 2009; 54:150–156. [PubMed: 19573732]
57. Fukushima K, Javadi MS, Higuchi T, et al. Prediction of short-term cardiovascular events using quantification of global myocardial flow reserve in patients referred for clinical ^{82}Rb PET perfusion imaging. J Nucl Med. 2011; 52:726–732. [PubMed: 21498538]
58. Ziadi MC, Dekemp RA, Williams KA, et al. Impaired myocardial flow reserve on rubidium-82 positron emission tomography imaging predicts adverse outcomes in patients assessed for myocardial ischemia. J Am Coll Cardiol. 2011; 58:740–748. [PubMed: 21816311]
59. Schindler TH, Nitzsche EU, Schelbert HR, et al. Positron emission tomography–measured abnormal responses of myocardial blood flow to sympathetic stimulation are associated with the risk of developing cardiovascular events. J Am Coll Cardiol. 2005; 45:1505–1512. [PubMed: 15862426]
60. Di Carli MF, Hachamovitch R. New technology for noninvasive evaluation of coronary artery disease. Circulation. 2007; 115:1464–1480. [PubMed: 17372188]
61. Javadi MS, Lautamaki R, Merrill J, et al. Definition of vascular territories on myocardial perfusion images by integration with true coronary anatomy: A hybrid PET/CT analysis. J Nucl Med. 2010; 51:198–203. [PubMed: 20080895]
62. Rispler S, Keidar Z, Ghersin E, et al. Integrated single-photon emission computed tomography and computed tomography coronary angiography for the assessment of hemodynamically significant coronary artery lesions. J Am Coll Cardiol. 2007; 49:1059–1067. [PubMed: 17349885]
63. Groves AM, Speechly-Dick ME, Kayani I, et al. First experience of combined cardiac PET/64-detector CT angiography with invasive angio-graphic validation. Eur J Nucl Med Mol Imaging. 2009; 36:2027–2033. [PubMed: 19618180]
64. Santana CA, Folks RD, Garcia EV, et al. Quantitative (82)Rb PET/CT: Development and validation of myocardial perfusion database. J Nucl Med. 2007; 48:1122–1128. [PubMed: 17574973]
65. Kaster T, Mylonas I, Renaud JM, et al. Accuracy of low-dose rubidium-82 myocardial perfusion imaging for detection of coronary artery disease using 3D PET and normal database interpretation. J Nucl Cardiol. 2012; 19:1135–1145. [PubMed: 22996831]
66. Schinkel AF, Bax JJ, Poldermans D, et al. Hibernating myocardium: Diagnosis and patient outcomes. Curr Probl Cardiol. 2007; 32:375–410. [PubMed: 17560992]
67. Camici PG, Prasad SK, Rimoldi OE. Stunning, hibernation, and assessment of myocardial viability. Circulation. 2008; 117:103–114. [PubMed: 18172050]
68. Desideri A, Cortigiani L, Christen AI, et al. The extent of perfusion-F18-fluorodeoxyglucose positron emission tomography mismatch determines mortality in medically treated patients with chronic ischemic left ventricular dysfunction. J Am Coll Cardiol. 2005; 46:1264–1269. [PubMed: 16198841]
69. Einstein AJ, Moser KW, Thompson RC, et al. Radiation dose to patients from cardiac diagnostic imaging. Circulation. 2007; 116:1290–1305. [PubMed: 17846343]
70. Slomka PJ, Dey D, Duvall WL, et al. Advances in nuclear cardiac instrumentation with a view towards reduced radiation exposure. Curr Cardiol Rep. 2012; 14:208–216. [PubMed: 22327929]
71. Lee DC, Simonetti OP, Harris KR, et al. Magnetic resonance versus radionuclide pharmacological stress perfusion imaging for flow-limiting stenoses of varying severity. Circulation. 2004; 110:58–65. [PubMed: 15210596]
72. Al-Saadi N, Nagel E, Gross M, et al. Noninvasive detection of myocardial ischemia from perfusion reserve based on cardiovascular magnetic resonance. Circulation. 2000; 101:1379–1383. [PubMed: 10736280]
73. Schwitter J, Wacker CM, van Rossum AC, et al. MR-IMPACT: Comparison of perfusion-cardiac magnetic resonance with single-photon emission computed tomography for the detection of

coronary artery disease in a multicentre, multivendor, randomized trial. Eur Heart J. 2008; 29:480–489. [PubMed: 18208849]

74. Nagel E, Lehmkuhl HB, Bocksch W, et al. Noninvasive diagnosis of ischemia-induced wall motion abnormalities with the use of high-dose dobutamine stress MRI: Comparison with dobutamine stress echocardiography. Circulation. 1999; 99:763–770. [PubMed: 9989961]
75. Nandalur KR, Dwamena BA, Choudhri AF, et al. Diagnostic performance of stress cardiac magnetic resonance imaging in the detection of coronary artery disease: A meta-analysis. J Am Coll Cardiol. 2007; 50:1343–1353. [PubMed: 17903634]
76. Wilke N, Jerosch-Herold M, Wang Y, et al. Myocardial perfusion reserve: Assessment with multisection, quantitative, first-pass MR imaging. Radiology. 1997; 204:373–384. [PubMed: 9240523]
77. Rieber J, Huber A, Erhard I, et al. Cardiac magnetic resonance perfusion imaging for the functional assessment of coronary artery disease: A comparison with coronary angiography and fractional flow reserve. Eur Heart J. 2006; 27:1465–1471. [PubMed: 16720685]
78. Costa MA, Shoemaker S, Futamatsu H, et al. Quantitative magnetic resonance perfusion imaging detects anatomic and physiologic coronary artery disease as measured by coronary angiography and fractional flow reserve. J Am Coll Cardiol. 2007; 50:514–522. [PubMed: 17678734]
79. Schwitter J, Nanz D, Kneifel S, et al. Assessment of myocardial perfusion in coronary artery disease by magnetic resonance: A comparison with positron emission tomography and coronary angiography. Circulation. 2001; 103:2230–2235. [PubMed: 11342469]
80. Jahnke C, Nagel E, Gebker R, et al. Prognostic value of cardiac magnetic resonance stress tests adenosine stress perfusion and dobutamine stress wall motion imaging. Circulation. 2007; 115:1769–1776. [PubMed: 17353441]
81. Coelho-Filho OR, Seabra LF, Mongeon FP, et al. Stress myocardial perfusion imaging by CMR provides strong prognostic value to cardiac events regardless of patient's sex. JACC Cardiovasc Imaging. 2011; 4:850–861. [PubMed: 21835377]
82. Kelle S, Chiribiri A, Vierecke J, et al. Long-term prognostic value of dobutamine stress CMR. JACC Cardiovasc Imaging. 2011; 4:161–172. [PubMed: 21329901]
83. Kellman P, Arai AE. Imaging sequences for first pass perfusion—A review. J Cardiovasc Magn Reson. 2007; 9:525–537. [PubMed: 17365232]
84. Schreiber WG, Schmitt M, Kalden P, et al. Dynamic contrast-enhanced myocardial perfusion imaging using saturation-prepared TrueFISP. J Magn Reson Imaging. 2002; 16:641–652. [PubMed: 12451577]
85. Di Bella EV, Parker DL, Sinusas AJ. On the dark rim artifact in dynamic contrast-enhanced MRI myocardial perfusion studies. Magn Reson Med. 2005; 54:1295–1299. [PubMed: 16200553]
86. Storey P, Chen Q, Li W, et al. Band artifacts due to bulk motion. Magn Reson Med. 2002; 48:1028–1036. [PubMed: 12465113]
87. Motwani M, Jogiya R, Kozerke S, et al. Advanced cardiovascular magnetic resonance myocardial perfusion imaging: High-spatial resolution versus 3-dimensional whole-heart coverage. Circ Cardiovasc Imaging. 2013; 6:339–348. [PubMed: 23512780]
88. Gerber BL, Rochitte CE, Bluemke DA, et al. Relation between Gd-DTPA contrast enhancement and regional inotropic response in the periphery and center of myocardial infarction. Circulation. 2001; 104:998–1004. [PubMed: 11524392]
89. Kim RJ, Albert TS, Wible JH, et al. Performance of delayed-enhancement magnetic resonance imaging with gadoversetamide contrast for the detection and assessment of myocardial infarction: An international, multicenter, double-blinded, randomized trial. Circulation. 2008; 117:629–637. [PubMed: 18212288]
90. Kim RJ, Shah DJ, Judd RM. How we perform delayed enhancement imaging. J Cardiovasc Magn Reson. 2003; 5:505–514. [PubMed: 12882082]
91. Kanal E, Barkovich AJ, Bell C, et al. ACR guidance document for safe MR practices: 2007. AJR Am J Roentgenol. 2007; 188:1447–1474. [PubMed: 17515363]
92. Kato S, Kitagawa K, Ishida N, et al. Assessment of coronary artery disease using magnetic resonance coronary angiography: A national multicenter trial. J Am Coll Cardiol. 2010; 56:983–991. [PubMed: 20828652]

93. Bogaert J, Kuzo R, Dymarkowski S, et al. Coronary artery imaging with real-time navigator three-dimensional turbo-field-echo MR coronary angiography: Initial experience. Radiology. 2003; 226:707–716. [PubMed: 12601209]
94. Schuijf JD, Bax JJ, Shaw LJ, et al. Meta-analysis of comparative diagnostic performance of magnetic resonance imaging and multislice computed tomography for noninvasive coronary angiography. Am Heart J. 2006; 151:404–411. [PubMed: 16442907]
95. Schuetz GM, Zacharopoulou NM, Schlattmann P, et al. Meta-analysis: Noninvasive coronary angiography using computed tomography versus magnetic resonance imaging. Ann Intern Med. 2010; 152:167–177. [PubMed: 20124233]
96. Kawasaki T, Koga S, Koga N, et al. Characterization of hyperintense plaque with noncontrast T1-weighted cardiac magnetic resonance coronary plaque imaging: Comparison with multislice computed tomography and intravascular ultrasound. JACC Cardiovasc Imaging. 2009; 2:720–728. [PubMed: 19520342]
97. Schoenhagen P, Ziada KM, Kapadia SR, et al. Extent and direction of arterial remodeling in stable versus unstable coronary syndromes: An intravascular ultrasound study. Circulation. 2000; 101:598–603. [PubMed: 10673250]
98. Ehara S, Hasegawa T, Nakata S, et al. Hyperintense plaque identified by magnetic resonance imaging relates to intracoronary thrombus as detected by optical coherence tomography in patients with angina pectoris. Eur Heart J Cardiovasc Imaging. 2012; 13:394–399. [PubMed: 22277117]
99. Schelbert HR. Quantification of myocardial blood flow: What is the clinical role? Cardiol Clin. 2009; 27:277–289. [PubMed: 19306770]

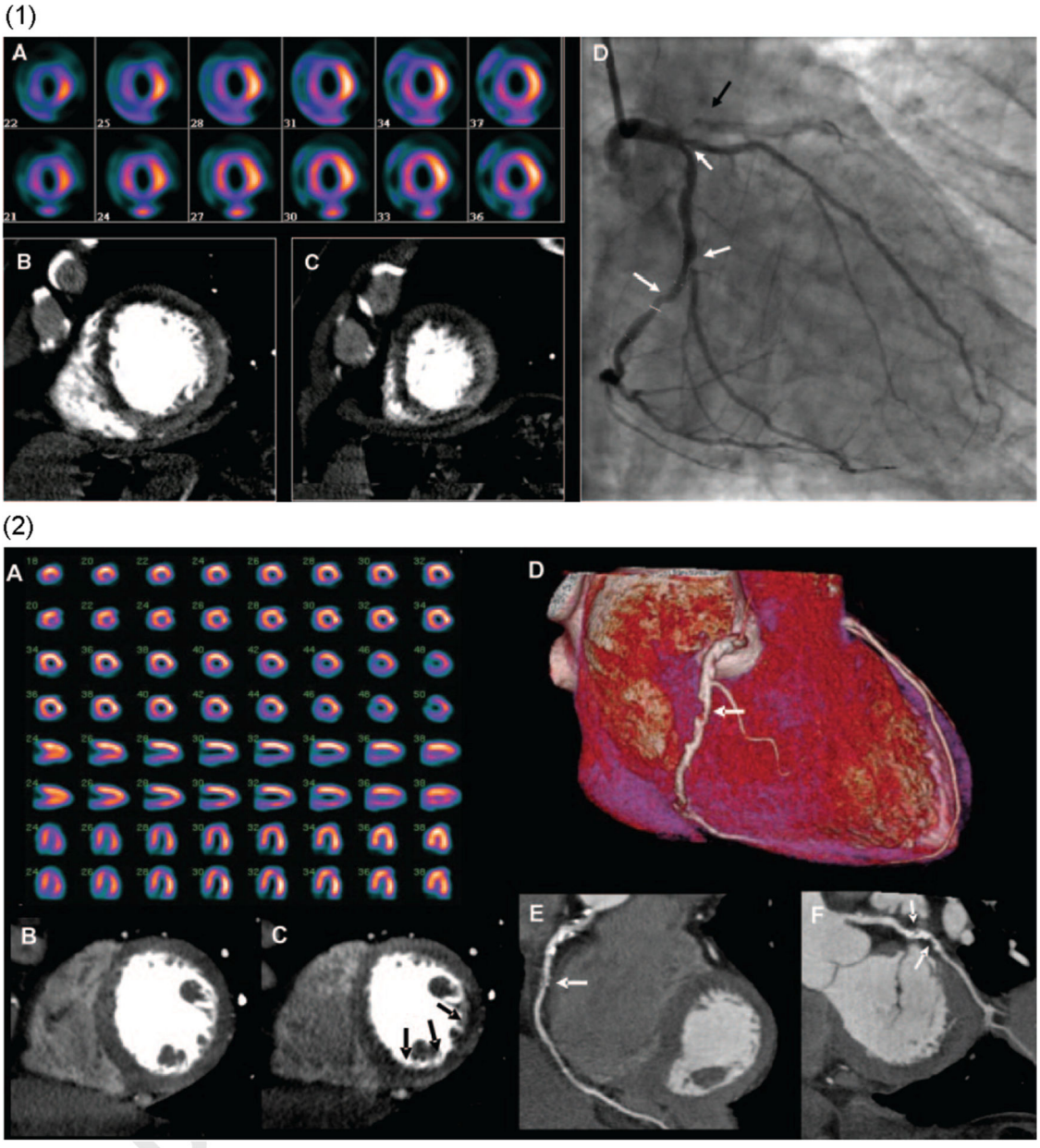

Figure 1.

(1) Images from a 64-row detector CTP. (A) A partially reversible perfusion deficit in the territory of the LAD and a primarily fixed perfusion deficit in the inferior wall on radionuclide myocardial perfusion imaging with increased subdiaphragmatic tracer uptake (stress, upper panels; rest, lower panels). (B and C) Adenosine stress CTP shows a dense perfusion deficit in the LAD territory and a subendocardial perfusion deficit in the inferior and lateral walls. (D) An invasive coronary angiogram demonstrates a left-dominant system with a totally occluded LAD (black arrow) as well as intermediate- and high-grade stenoses in a large ramus intermedius, the body of the left circumflex, and the ostium of the obtuse marginal artery (white arrows). (2) Images from a 256-row detector CTP. (A) A partially reversible perfusion deficit in the inferior and inferolateral wall on radionuclide MPI in this

patient with exertional angina (stress, upper panels; rest, lower panels). Rest (B) and stress (C) CTP imaging shows a reversible subendocardial perfusion deficit in the inferior and inferolateral walls. Noninvasive angiography confirms a significant stenosis (white arrows) in the proximal right coronary artery (D and E) and the proximal left circumflex artery (F).[27] (Color version of figure is available online.)

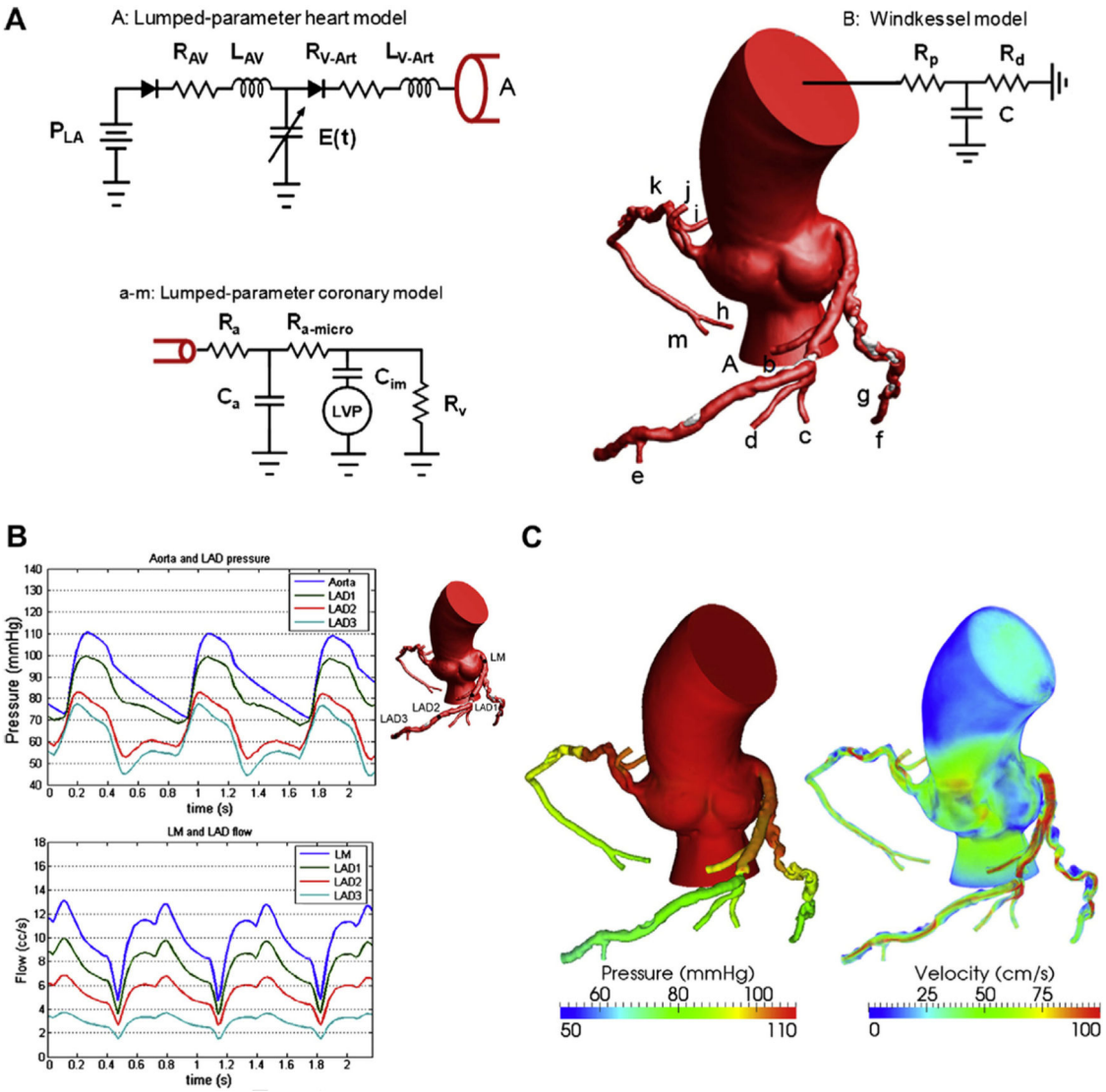

Figure 2.

A mathematical model for pulsatile coronary flow. (A) Lumped parameter models are coupled to the aortic inlet and noncoronary vasculature and coronary microcirculation. P is the pressure, R the resistance, C the capacitance, L the inductance, and E(t) the elastance. Subscript LA is for the left atrium, AV for atrioventricular, V-Art for ventricle-arterial, p for proximal, d for distal, a for arterial, im for intermyocardial, and V for venous. (B) Pulsatile pressure and flow rate waveforms demonstrate reduced coronary flow in early systole because of contraction of the ventricle followed by increased flow in diastole, resulting from relaxation of the ventricle. (C) Velocity fields and 3-dimensional pressure are computed throughout the cardiac cycle. The pressure gradients and high-velocity jets across stenoses in the left anterior descending artery (LAD), left circumflex artery (LCX), and right coronary artery (RCA) can be noted.[32] (Color version of figure is available online.)

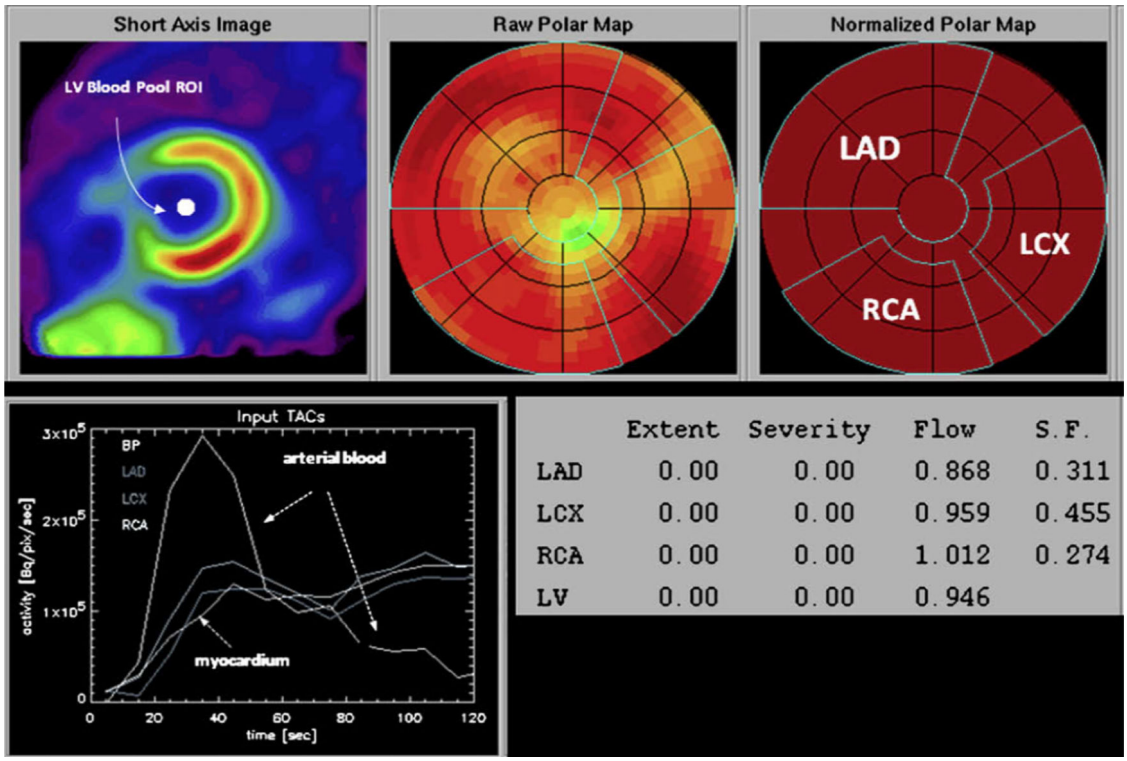

Figure 3.

Determination of regional myocardial blood flow from the serially acquired PET images. On the reoriented short-axis image of the left ventricular myocardium (upper left panel), a region of interest is assigned to the left ventricular blood pool. The polar map displays the relative distribution of the flow tracer throughout the left ventricular myocardium. Based on a comparison with a normal database, no regional reductions in radiotracer activity are identified. Regions of interest are assigned to the territories of the left anterior descending (LAD), the left circumflex (LCX), and the right coronary arteries (RCAs). The corresponding time-activity curves for arterial blood and the myocardial regions are shown in the left lower panel. The final readout is shown in the lower left panel; extent and severity of regional flow defects are indicated but listed as zero because of the normal homogenous radiotracer distribution. Values of flow in mL/min/g are indicated for each of the vascular territories as well as the entire left ventricular myocardium. ROI, region of interest; S.F., spillover fraction, for cross contamination of activity from blood into myocardium.[99] (Color version of figure is available online.)

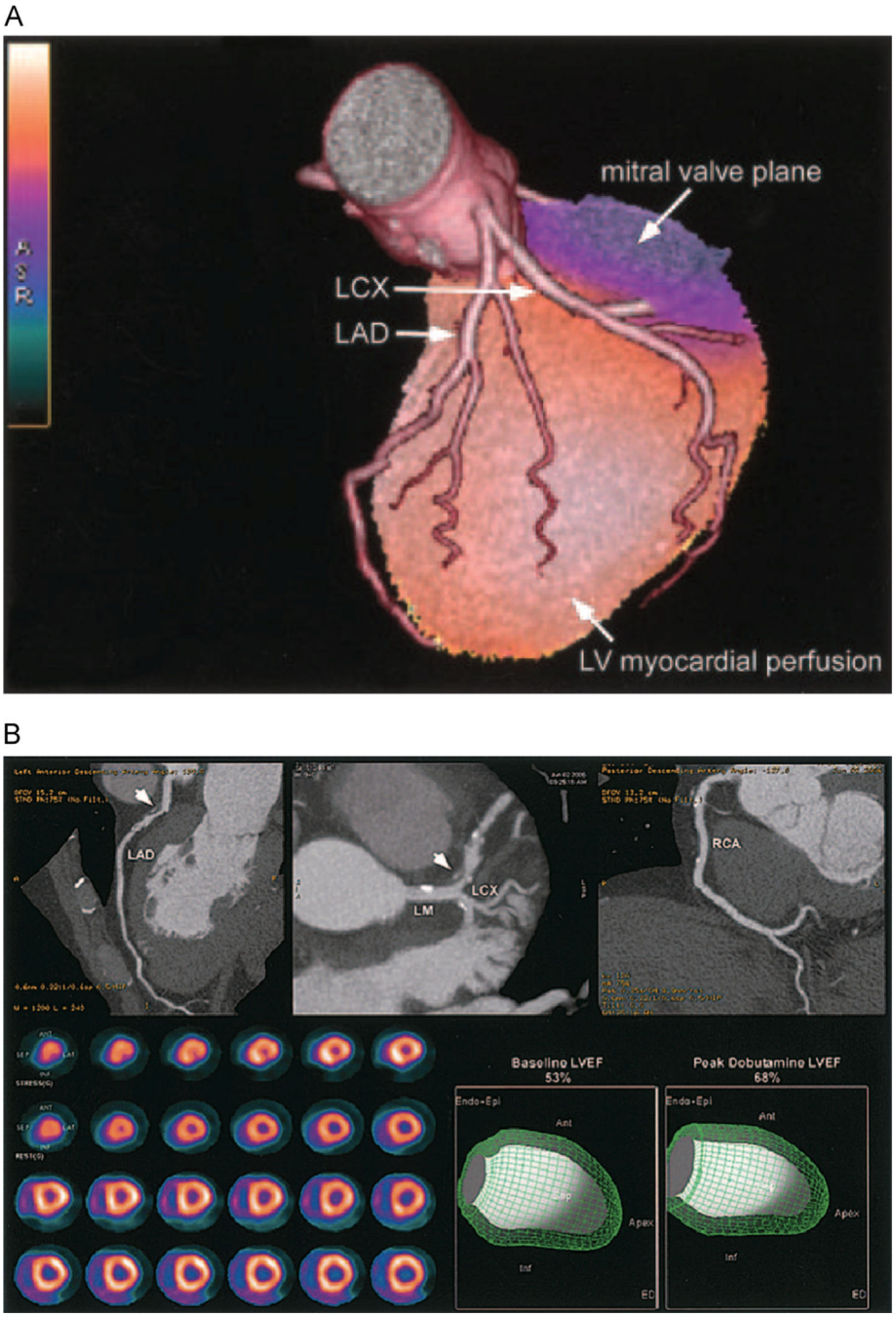

Figure 4.

(A) Fused 3D reconstructions of a coronary arteriogram and stress myocardial perfusion obtained in the same setting, assessed through integrated PET/CT. A full-motion cine can be viewed in the online-only Data Supplement Movie V. LCX indicates left circumflex artery; LAD, left anterior descending coronary artery.[60] (B) An integrated PET/CT study. The CTA images demonstrate a noncalcified plaque (arrowhead) in the proximal left anterior descending coronary artery (LAD) with 50%-70% stenosis; however, the rest and peak dobutamine stress myocardial perfusion PET study (lower left panel) demonstrates only

minimal inferoapical ischemia. In addition, LVEF was normal at rest and demonstrated a normal rise during peak dobutamine stress. Full-motion cines can be viewed in the online-only Data Supplement (Movies VI and VII). Ant, anterior; Endo Epi, endocardial plus epicardial; Inf, inferior; LCX, left circumflex; LM, left main; RCA, right coronary artery.[60]